REPORT DOCUMENTATION PAGE

Form Approved
OMB No. 0704-0188

1. REPORT DATE *(DD-MM-YYYY)*	2. REPORT TYPE	3. DATES COVERED *(From - To)*
	Technical Paper	

4. TITLE AND SUBTITLE

5a. CONTRACT NUMBER

5b. GRANT NUMBER

5c. PROGRAM ELEMENT NUMBER
62500F

6. AUTHOR(S)

5d. PROJECT NUMBER
2308

5e. TASK NUMBER
M4S7

5f. WORK UNIT NUMBER
345382

7. PERFORMING ORGANIZATION NAME(S) AND ADDRESS(ES)

8. PERFORMING ORGANIZATION REPORT

9. SPONSORING / MONITORING AGENCY NAME(S) AND ADDRESS(ES)

Air Force Research Laboratory (AFMC)
AFRL/PRS
5 Pollux Drive.
Edwards AFB CA 93524-7048

10. SPONSOR/MONITOR'S ACRONYM(S)

11. SPONSOR/MONITOR'S NUMBER(S)

12. DISTRIBUTION / AVAILABILITY STATEMENT

Approved for public release; distribution unlimited.

13. SUPPLEMENTARY NOTES

See attached 13 papers, all with the information on this page.

14. ABSTRACT

15. SUBJECT TERMS

16. SECURITY CLASSIFICATION OF:			17. LIMITATION OF ABSTRACT	18. NUMBER OF PAGES	19a. NAME OF RESPONSIBLE PERSON
					Kenette Gfeller
a. REPORT	b. ABSTRACT	c. THIS PAGE	A		19b. TELEPHONE NUMBER *(include area code)*
Unclassified	Unclassified	Unclassified			(661) 275-5016

Microinstabilities in a 10-Kilowatt Self-Field Magnetoplasmadynamic Thruster

Dennis L. Tilley, Edgar Y. Choueiri,
Arnold J. Kelly, Robert G. Jahn

Reprinted from

Journal of Propulsion and Power

Volume 12, Number 2, Pages 381–389

AIAA

A publication of the
American Institute of Aeronautics and Astronautics, Inc.
370 L'Enfant Promenade, SW
Washington, DC 20024-2518

JOURNAL OF PROPULSION AND POWER
Vol. 12, No. 2, March–April 1996

Microinstabilities in a 10-Kilowatt Self-Field Magnetoplasmadynamic Thruster

Dennis L. Tilley,* Edgar Y. Choueiri,† Arnold J. Kelly,‡ and Robert G. Jahn§
Princeton University, Princeton, New Jersey 08544

Theoretical studies indicate that a variety of microscopic and macroscopic plasma instabilities can significantly affect the performance of the magnetoplasmadynamic (MPD) thruster, yet experimental evidence for their existence is extremely limited. The objective of this research was to provide experimental evidence for the existence of microinstabilities in a 10-kW-class, self-field MPD thruster. The lower-bound of the range of thruster operating currents investigated in this study was set by the requirement that the electromagnetic thrust component be much greater than the electrothermal thrust component. The upper-bound of the operating current was set by the initial observation of high-frequency thruster voltage oscillations, which is usually associated with the onset of excessive thruster erosion. Experimental evidence for two microinstabilities was obtained in the near-field plume of the thruster: 1) the generalized lower hybrid drift instability and 2) the electron cyclotron drift instability.

Nomenclature

B = magnetic field
D = thruster exit plane diameter
e = charge of an electron
f = frequency, Hz
f_{max} = frequency corresponding to maximum growth of the generalized lower hybrid drift instability in the lab frame
f_N = Nyquist frequency
f_n = frequency corresponding to maximum growth of the electron cyclotron drift instability in the lab frame
J = current density
J_t = thruster current level
k = wave vector, $2\pi/\lambda$, λ = wavelength
L_x = characteristic gradient scale length of $x \equiv [\nabla(\ell n\, x)]^{-1}$
M_i = ion mass
m = frequency averaging number
$\dot{m}$ = thruster mass flow rate
m_e = electron mass
n = harmonic number, 1, 2, 3, ...
n_e = electron number density
r, θ, z = radial, azimuthal, and axial coordinate
r_L = Larmor radius $\equiv V_t/\Omega$
r_p = probe radius
S_{11} = power spectrum
T = temperature
U = drift velocity
V_{d2} = triple probe voltage
V_t = thermal velocity $\equiv (2\kappa T/M)^{1/2}$
V_ϕ = phase velocity
β_e = plasma beta $\equiv 2\mu_0 n_e \kappa T_e/B^2$
κ = Boltzmann constant
λ_d = electron Debye length
ν = collision frequency
Ω = electron or ion cyclotron frequency $\equiv eB/M$
ω = angular frequency, rad/s, $\equiv 2\pi f$
ω_{LH} = lower hybrid frequency $\cong (\Omega_e \Omega_i)^{1/2}$
ω_p = electron or ion plasma frequency $\equiv (ne^2/\varepsilon_0 M)^{1/2}$

Subscripts
e = electron
i = ion

Superscript
$*$ = property at maximum growth rate

I. Introduction

THE magnetoplasmadynamic (MPD) thruster is a space propulsion device that utilizes the $\boldsymbol{J} \times \boldsymbol{B}$ force to accelerate a plasma to exhaust velocities useful for missions in space (10–50 km/s).[1] Currently, the MPD thruster is not efficient enough to make it a viable option for missions of current interest. Typical maximum efficiencies are in the 20–40% range, while a minimum of 60% is required for the MPD thruster to become competitive with chemical and other electric propulsion devices.[2] In 1988, Choueiri et al.[3] suggested that current-driven microscopic plasma instabilities (i.e., microturbulence) may play an important role in the inefficient operation of the MPD thruster. Current-driven microturbulence counters the objective of the MPD thruster, which is to push the propellant, by taking much of the energy available for acceleration and converting it into various unrecoverable energy modes, such as those associated with thermal motion, ionization, excitation, and radiation. This suggestion provided the impetus for this study of microinstabilities in a 10-kW-class, self-field MPD thruster.

An enormous body of literature is dedicated to the study of instabilities in plasmas containing a current perpendicular to a magnetic field.[4] There exists a fair amount of research on the effect of plasma instabilities on other electromagnetic acceleration devices utilizing $\boldsymbol{J} \times \boldsymbol{B}$ forces (e.g., the Hall current accelerator[5]). While studies of plasma instabilities in Hall current accelerators and other plasma physics apparatus are helpful to MPD thruster research, they are not strictly applicable,

Received June 8, 1992; revision received July 17, 1994; accepted for publication Aug. 25, 1995.

*Graduate Student, Electric Propulsion and Plasma Dynamics Laboratory; currently at Phillips Laboratory, Electric Propulsion Group, Edwards Air Force Base, CA. Member AIAA.

†Research Associate, Electric Propulsion and Plasma Dynamics Laboratory.

‡Senior Research Engineer, Electric Propulsion and Plasma Dynamics Laboratory. Member AIAA.

§Professor, Electric Propulsion and Plasma Dynamics Laboratory, Mechanical and Aeronautical Engineering Department. Fellow AIAA.

because the plasma properties in the MPD thruster differ significantly from those of other devices. The plasma internal to the MPD thruster is relatively dense and collisional such that the electron Hall parameter ranges from order 1 to order 10 and the plasma β ranges from much less than 1 to as high as order 10. In addition to the sheath regions, large gradients in plasma properties are typical inside the MPD thruster. Current densities and induced magnetic fields can span many orders of magnitude, up to ~10^3 A/cm^2 and ~1 kG in MW-level devices.[6,7] The plasma is typically highly ionized, with charged particle number densities in the 10^{13}–10^{16}/cm^3 range,[6–10] and is relatively isothermal, with the electron temperature T_e and ion temperature T_i on the order of 1 eV (Refs. 7–13). The unique combination of plasma properties in the MPD thruster necessitates its own theoretical and experimental investigation.

Initial work concerning the effects of plasma instabilities on MPD thruster performance focused on the prediction of the onset of various pathological thruster operation modes. Many instabilities have been invoked as the cause of the so-called onset current limitation, where high-frequency terminal voltage fluctuations and excessive erosion are observed when the thruster current exceeds a critical level. These include microscopic instabilities such as the Buneman, ion acoustic, and electron acoustic instabilities,[14,15] as well as macroscopic instabilities such as electrothermal instability[16,17] and others.[18–21] Experimentally, inconclusive attempts have been made to identify the instability associated with the onset current limitation by the examination of power spectra of both the terminal voltage and light intensity fluctuations.[22] In the case of an MPD thruster with an applied axial magnetic field, plasma instabilities have also been proposed as being responsible for the rotating spoke phenomenon.[23,24]

Only recently has the research emphasis shifted towards the investigation of the effects of microinstabilities on MPD thrusters operating at a current level below the onset current. Many observations support the view that microinstabilities do significantly affect MPD thruster performance. These include ionization fractions[9] and line radiation[25] levels much larger than what is expected classically, and the measurements of enhanced plasma resistivity.[11,26] Current research efforts include the theoretical identification of the various instabilities that may exist in the MPD thruster[3,17–21,27–30] and the calculation of their nonlinear effects on MPD thruster performance.[27,29,31–33] Presently, the focus has been placed on the investigation of the generalized lower hybrid drift instability (GLHDI),[34,35] because it is suspected that this microinstability most strongly affects the anomalous transport properties (e.g., resistivity, viscosity, and heat conduction) of the MPD thruster plasma.

Experimental verification of the existence of plasma instabilities in the MPD thruster plasma is extremely limited. Most notably, by measurement of the linear dispersion relation,[3] the plasma in the plume of an MW-level MPD thruster is indeed unstable to small density disturbances. In addition, recent dispersion relation measurements have provided evidence for the existence of the GLHDI in the same thruster.[30]

The objective of this work was to provide additional experimental data concerning the existence of microinstabilities in the self-field MPD thruster. Specifically, this study is concerned with the MPD thruster operating at a sufficient current level such that the electromagnetic thrust component is much greater than the electrothermal thrust component, but at a level below the onset current. To achieve this objective three separate experiments were performed. First, the plasma properties in a steady-state 10-kW MPD thruster plume were characterized using a triple probe and Hall probe. In the second experiment, the triple probe was used to investigate turbulent fluctuations of plasma properties, as a means to identify the presence of microinstabilities. In the last experiment, measurements of the plasma dispersion relation were used to provide further evidence for the identification of the microinstabilities present in the 10-kW MPD thruster plume.

This article is organized as follows. In Sec. II a brief review of the microinstabilities that may exist in the plasma of the MPD thruster is presented. In Sec. III the characterization of the 10-kW MPD thruster plume is discussed. The investigation of the turbulent fluctuations of plasma properties and the measurement of the plasma dispersion relation are discussed in Secs. IV and V, respectively. Finally, conclusions are presented in Sec. VI.

II. Brief Review of Microinstabilities that May Exist in the MPD Thruster Plasma

In view of the limited experimental evidence for the existence of microinstabilities in the MPD thruster, a brief review of those that may theoretically exist in the MPD thruster is presented. This review will also help to identify regions of frequency space most likely to reveal evidence of microinstabilities and to facilitate the interpretation of experimental results to be discussed later.

First, it is important to specify the regime of MPD thruster operation considered in this study, which can be characterized by the parameter $J_i^2/\dot{m}$. The lower-bound $J_i^2/\dot{m}$ is established by the requirement that the electromagnetic component of thrust be much greater than the electrothermal component. The upper-bound $J_i^2/\dot{m}$ is limited by that associated with the onset phenomenon. With these bounds, the minimum value of $J_i^2/\dot{m}$ is estimated to be ~20 kA^2 s/g for an MPD thruster operating with the propellant argon, whereas the maximum value depends on many parameters, but is typically (for argon) greater than 100 kA^2 s/g (Ref. 2). MPD thrusters are also commonly operated in regimes where the electrothermal thrust is comparable with the electromagnetic thrust.[36] In such a regime of operation, other macroscopic plasma instabilities, not considered in this study, may be excited in the MPD thruster.

In the previously stated operating regime, large current densities in the MPD thruster plasma constitute a large source of free energy to drive an instability. Experimental measurements have shown that the ratio of the electron drift velocity U_e to the ion thermal velocity V_{ti} typically ranges from 1 to 100 (Refs. 6–13). On this basis, and for the sake of simplicity, only current-driven microinstabilities will be the focus of this study. The number of microinstabilities to be considered is further reduced to those driven by a cross-field current, because the current density is always perpendicular to the magnetic field in the self-field MPD thruster.

Listed in Table 1 are five well-known microinstabilities driven by a cross-field current, along with their characteristics

Table 1 Five microinstabilities known to exist in a plasma with a cross-field current

Instability	Main condition for existence	Maximum growth characteristics in the ion rest frame	
GLHDI	Can exist for $U_e < V_{ti}$	$\omega^* \approx \omega_{LH}$	$k^* \leq r_{Le}^{-1}$
ECDI, $\omega^* \cong n\Omega_e$ in the electron frame	$U_e > V_{ti}$	$\omega^* \approx n\Omega_e[(U_e/V_{ti}) - 1]^{-1}$	$k^* \approx n\Omega_e(U_e - V_{ti})^{-1}$
Buneman instability, $\omega^* \cong \omega_{pe}$ in the electron frame	$U_e > V_{te}$	$\omega^* \approx (m_e/M_i)^{1/3}\omega_{pe}$	$k^* \approx \omega_{pe}/U_e$
Ion acoustic instability, $kr_{Le} >> 1$	$T_e >> T_i$, $U_e > (\kappa T_e/M_i)^{1/2}$	$\omega^* \approx \omega_{pi}$	$k^* \approx \lambda_d^{-1}$
Drift cyclotron instability	$(m_e/M_i)^{1/2} \leq (r_{Li}/L_x) \leq (m_e/M_i)^{1/4}$	$\omega^* \approx n\Omega_i$	$k^* \approx r_{Le}^{-1}$

at maximum growth (denoted by the asterisk) and their main condition for existence. Further details, such as the derivation of these characteristics, can be obtained in the references cited later in this article. Each instability operates near a natural frequency of the plasma, and each has its own effects on the plasma, in terms of anomalous transport. Microinstabilities requiring $T_i \gg T_e$ for existence, such as the electron acoustic instability,[37] have been eliminated from consideration, along with those microinstabilities that have a growth rate much smaller than the ion residence time in the thruster, e.g., the universal instabilities.[4]

The Buneman instability operates in both magnetized and unmagnetized plasmas near the electron plasma frequency (in the electron reference frame) and is excited when the electron drift velocity exceeds the electron thermal velocity.[35,38] Excluding the sheath regions, experiments in the MPD thruster have shown that the electron drift velocity is only a small fraction of the electron thermal velocity, effectively stabilizing the Buneman instability.

In a magnetized plasma, for $T_e >> T_i$, the ion acoustic instability operates in two regions of wave number space[35,39]: $kr_{Le} << 1$ (Ref. 37) and $kr_{Le} >> 1$. In the region of $kr_{Le} >> 1$, where significantly higher growth rates exist, the ion acoustic instability behaves as its nonmagnetic counterpart with $\omega^* \approx \omega_{pi}$ and $k^* \approx \lambda_d^{-1}$, where ω_{pi} is the ion plasma frequency. The general condition for existence of the ion acoustic instability is that $T_e/T_i >> 1$, which is generally not satisfied in the MPD thruster.[12,13] However, the ion acoustic instability cannot be eliminated from consideration altogether, because the stability criterion is very sensitive to the actual electron and ion velocity distribution functions. Furthermore, the presence of an electron temperature gradient has also been shown to destabilize ion acoustic waves in isothermal plasmas,[40] suggesting that the ion acoustic instability may operate near the centerline of the MPD thruster, off the tip of the cathode, where large T_e gradients exist.[9,10]

The drift cyclotron instability (DCI) (Ref. 41) operates at discrete frequencies near the harmonics of the ion cyclotron frequency ($n\Omega_i$, $n = 1, 2, \ldots$). The existence of the DCI depends on the gradient of various plasma properties (which create the cross-field current). The gradient scale length of property x, L_x [$\equiv 1/\nabla(\ell n\, x)$], must be sufficiently small to excite the instability, but not too small, for then the DCI will transform into the GLHDI at wave numbers near r_{Le}^{-1}. Collisions are also known to transform the DCI into the GLHDI (Ref. 42). In typical MPD thruster plasmas, the gradient scale lengths are generally much smaller than the ion Larmor radius, and the ion Hall parameter, which is the ratio of the ion cyclotron frequency to the ion–ion collision frequency, is typically much less than unity (typically: $\Omega_i/\nu_{ii} \sim 10^{-2}$). Therefore, the DCI is expected to be fully transformed into the GLHDI in the MPD thruster.

The GLHDI (Refs. 34 and 35), as its name implies, designates a general type of instability, where the detailed characteristics (ω and k) depend on many plasma parameters and their gradients, but has the general tendency to operate near the lower hybrid frequency. The GLHDI can be excited by relatively low-drift velocities and has been studied extensively in several more simplified forms, such as the modified two-stream instability,[28,37,39] the lower hybrid drift instability,[43] the kinetic cross-field streaming instability,[44] and the Farley–Buneman instability.[45] The magnitude and direction of k^* can vary significantly depending on the plasma conditions, such as the presence of gradients, collisions, and the value of the electron plasma beta β_e ($\equiv 2\mu_0 n_e k T_e/B^2$). The direction of k^* can be exactly perpendicular to the magnetic field or be on the order of 45 deg between the magnetic field and electron drift velocity vector; while the magnitude of k^* can be as large as the inverse electron gyroradius ($k^* r_{Le} \approx 1$) or be much smaller ($k^* r_{Le} << 1$). A review of the previous special cases and their application to the MPD thruster plasma is presented in Ref. 29. The GLHDI apparently has no fundamental restrictions forbidding its existence in the MPD thruster. Even in the highly collisional plasma of the MPD thruster, the GLHDI can be excited, although it behaves somewhat differently than the collisionless GLHDI (Ref. 29).

In the electron reference frame, the electron cyclotron drift instability (ECDI) (Refs. 46 and 47) operates at discrete frequencies near the harmonics of the electron cyclotron frequency ($n\Omega_e$ and $n = 1, 2, \ldots$). The typical unstable wavelength is much shorter than the electron gyroradius ($k^* r_{Le} >> 1$), and is directed essentially perpendicular to the magnetic field, in the direction of the electron drift velocity. The ECDI, like the GLHDI, has no fundamental restrictions forbidding its existence in the MPD thruster.

In summary, excluding unusual circumstances in which the ion acoustic instability is excited, it is anticipated that two microinstabilities are most likely to be present in the MPD thruster plasma: 1) the GLHDI and 2) the ECDI. The focus of the experiments in this work was to obtain evidence for the existence of these microinstabilities in a 10-kW MPD thruster.

III. Characterization of the 10-kW MPD Thruster Plume

Knowledge of various plasma properties is essential for any experimental investigation of plasma instabilities. With the measurements of n_e, T_e, the azimuthal magnetic field B_θ, and the current density J, it is possible to calculate most of the relevant plasma properties required to investigate the stability of the MPD thruster plasma. In this section, the results of the plasma property characterization in the plume of the 10-kW MPD thruster are presented.

All experiments were conducted in the near-field plume of a steady-state 10-kW-class MPD thruster; i.e., with $z/D < 1$, where z is the axial distance downstream from the exit plane. The fact that these experiments were not conducted inside of the thruster did not severely limit the scope of this investigation; many studies have shown that significant electromagnetic interactions, characteristic of inside of the MPD thruster, can occur in the plume (e.g., Ref. 48). Moreover, concerning the question of the existence of microinstabilities, it has been suggested that the plasma in the plume is quite similar to that inside the MPD thruster.[49]

The experiments were conducted in the Princeton 30-kW steady-state thruster facility.[9,50] The vacuum tank is 1.5 m in diameter, 6.4 m long, evacuated by one 1.2-m diffusion pump, and backed by a Roots blower and a mechanical pump. With this pumping system the tank pressure during thruster operation was less than 5×10^{-4} torr. Probe positioning was achieved by a pendulum arm mechanism, which swept the probes through the plume,[49] allowing for radial profiles of the plasma properties to be obtained. The steady-state MPD thruster used in this research is shown schematically in Fig. 1.

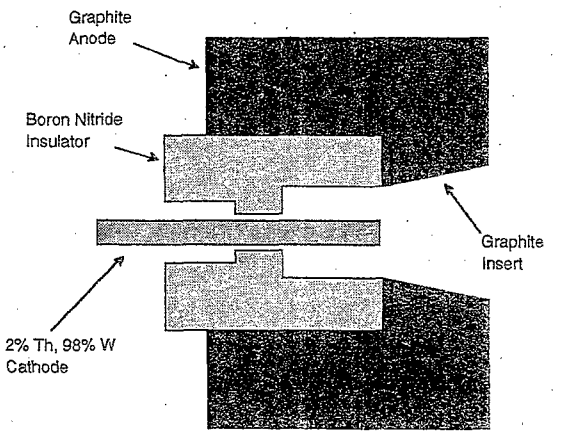

Fig. 1 Scale schematic of the steady-state 10-kW self-field MPD thruster.

The thruster has coaxial geometry, a 2% thoriated tungsten 0.64-cm-diam cathode, a graphite anode insert with an exit diameter of 3.5 cm enclosed in a graphite cylinder 10 cm in diameter. The plumbing and electrical connections, located behind the thruster, are described in Ref. 50. The thruster was powered by a modified 50-kW welding supply with a maximum ripple factor of 0.5%. Experiments were performed approximately 30–60 s after ignition to allow the thruster to equilibrate thermally. Typical operating conditions with the propellant argon are currents from 500–900 A, mass flow rates in the 8–13 mg/s range, and terminal voltages of 20–30 V.

A triple probe[51] was employed to measure the electron temperature and electron number density of the plasma. The triple probe is capable of making essentially instantaneous measurements of T_e and n_e, allowing for the attainment of an entire radial profile in a single swing of the pendulum arm through the plume. The triple probe consisted of three cylindrical electrodes configured in a three-in-line fashion (the electrode spacing was 1 mm, the r_p was 0.121 mm, and the electrode length was 5 mm).[49] The thin sheath limit criterion, which applies for $r_p/\lambda_d > 100$, was not satisfied in the plume of the 10-kW thruster (typically, $r_p/\lambda_d \sim 10$–30). Therefore, a modification of the triple-probe theory,[10] based on the calculations of Laframboise,[52] was utilized. Using this theory, T_e and n_e were calculated from the two triple-probe outputs: 1) the voltage V_{dz} and 2) the current. In these calculations it was assumed that $T_i = T_e$ and that the ion species were singly ionized. The effect of ions drifting perpendicular to the triple probe, known to significantly affect triple-probe performance,[10] was accounted for by aligning the triple probe with the ion flow vector as discussed in Refs. 10 and 49. The uncertainty associated with the triple-probe measurements was estimated to be ≈10% for T_e and ≈60% for n_e, due to unknown ion temperature, unknown species composition, and because of the existence of a nonzero electron drift velocity perpendicular to the probe.[10]

In Figs. 2 and 3, three radial profiles of electron temperature and electron number density in the near-field plume of the 10-kW thruster are shown. The T_e profiles, shown in Fig. 2, are very similar in shape and magnitude to spectroscopic measurements obtained by Myers[9] at the exit plane of the same thruster. Both indicate a relatively flat profile of T_e, except near the centerline. The magnitudes of the number density measurements, shown in Fig. 3, were also consistent with spectroscopic measurements obtained at the exit plane by Myers.[9] The effect of mass flow rate on T_e is small, while n_e is observed to increase slightly with increasing mass flow rate, as observed in other MPD thrusters.[53] Note that the triple-probe output was not filtered, indicating that the plasma was not grossly turbulent at these operating conditions.

Measurements of the azimuthal magnetic field and current density in the plume of the 10-kW thruster were obtained by the use of a Hall-effect probe.[54] It consisted of two Hall generators, displaced axially such that a radial profile of B_θ and dB_θ/dz could be obtained.[49] The axial and radial current densities, used to derive the electron drift velocity with respect to the ions ($U_e = J/n_e e$), were then calculated via Maxwell's equations. Figure 4 shows typical measurements of the azimuthal magnetic field at an axial location of 1.7 cm downstream of the exit plane, at a mass flow rate of 10 mg/s, as the thruster current is varied. It was observed that the magnetic fields were strongly affected by the thruster current level, while being relatively insensitive to mass flow rate variations. The small hump occurring near $r = +5$ cm, caused by mechanical factors, was eliminated in the experiments to be discussed in Secs. IV and V.

The largest source of error in the magnetic field measurements is due to the uncertainty of the location of the probe ($\Delta r = \pm 0.5$ steps = 1.3 mm). Depending on the region of the plume, the uncertainty in the magnetic field measurement was typically 10–25% and no less than 3%, which was the calibration uncertainty. For radii less than 0.75 cm, it is also expected that the probe will significantly perturb the magnetic field by inhibiting the current inducing B_θ (Ref. 49). Therefore, in the experiments to be discussed later, only measurements from the $r > 0.75$-cm region of the plume and from reasonably symmetric profiles were considered reliable. Typically, in the region $r > 0.75$, axial current densities ranged from 1 to 10 A/cm^2, while maximum radial current densities were in the 1–4 A/cm^2 range. Typical uncertainties in these calculations, because of the uncertainty in the position of the probe, were 25–50%.

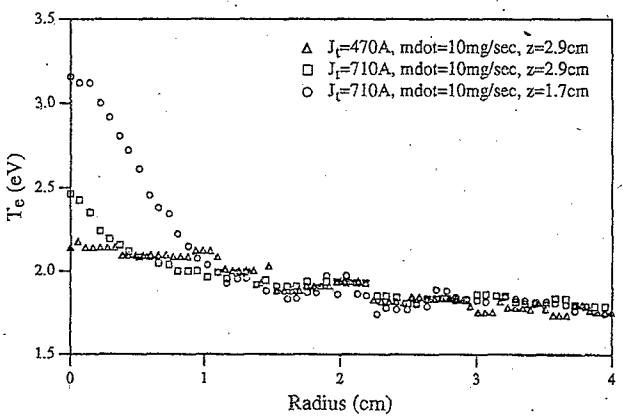

Fig. 2 Typical radial profiles of electron temperature in the near-field plume of the 10-kW MPD thruster (uncertainty in the measurements was ≈10%).

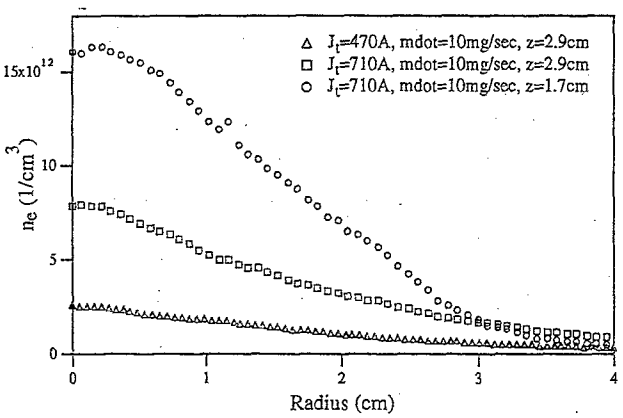

Fig. 3 Typical radial profiles of electron number density in the near-field plume of the 10-kW MPD thruster (uncertainty of the measurements was ≈60%).

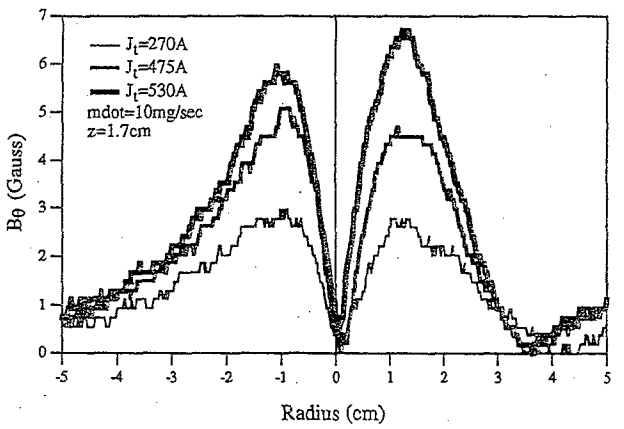

Fig. 4 Typical radial profiles of the azimuthal magnetic field in the near-field plume of the 10-kW MPD thruster.

IV. Investigation of Turbulent Power Spectra

The rationale behind this experiment stems from the assumption that each microinstability listed in Table 1 operates near a different natural frequency of the plasma. By measuring the power spectrum of naturally occurring plasma fluctuations and comparing it with measured natural frequencies (f_{ci}, f_{LH}, f_{ce}, f_{pi}, and f_{pe}), it is possible to obtain evidence indicating that microinstabilities are present in the MPD thruster plasma. Previous researchers, in an attempt to identify plasma instabilities, have investigated the power spectra of both the MPD thruster's terminal voltage and light intensity measurements from the plume, without the concurrent measurement of the natural plasma frequencies.[22] Moreover, the terminal voltage and light intensity measurements in that work were integrated over space, which make them extremely difficult to use for the identification of plasma instabilities. This experiment differs from past research in that the frequency content of the local plasma property fluctuations are measured and compared with measurements of local natural frequencies, allowing for a much clearer interpretation of the spectra.

Three main assumptions form the basis for this approach. The first assumption, consistent with the reasoning in Sec. II, is that Table 1 represents an extensive list of all microinstabilities that may be excited in the MPD thruster (operating at sufficiently high $J_t^2/\dot{m}$). Second, the characteristics of each microinstability listed in Table 1 are approximately correct for the plasma of the 10-kW thruster plume, where β_e is generally much larger than one. This assumption is reasonable, considering that theoretical studies have shown that the characteristics of the GLHDI (Refs. 29 and 30) and the ECDI (Ref. 55) do not change much as β_e approaches unity. While it is true that β_e does affect k^*, ω^*, and the stability of the microinstabilities listed in Table 1, only order-of-magnitude estimates of k^* and ω^* are required to interpret the data. This is the case because the following condition applies to the plasma in the plume of the 10-kW MPD thruster: $f_{ci} << f_{LH} << f_{ce} << f_{pi} << f_{pe}$. The third assumption is that the location of the peak in the power spectra is approximately equal to the frequency corresponding to the maximum linear growth rate. Such an assumption is reasonable because it is commonly observed that saturated-state plasma fluctuations still retain much of their linear characteristics.[56]

The triple probe was the primary means by which plasma property fluctuations were measured. The fluctuations of V_{d2} reflect essentially fluctuations of T_e and the electric field component along the electrodes, whereas fluctuations of the current reflect essentially number density and electron temperature fluctuations.[49] The natural plasma frequencies were obtained by simultaneously sweeping the triple probe and the Hall probe through the plume of the thruster. The triple probe was aligned with the thruster axis; consequently, the uncertainty of the measurements increased because it was no longer aligned with the ion flow vector in all regions of the plume. The uncertainty of the measurements was estimated to be ≈25% for T_e and approximately a factor of 2 for n_e (Ref. 10).

A Nicolet 320 digital oscilloscope, sampling at 5 MHz, recorded the triple-probe outputs, resulting in the maximum observable frequency, the Nyquist frequency f_N of 2.5 MHz. Of the 4000 data points obtained by the digital oscilloscope, 2048 were used for data analysis such that a 2^{11} data point fast Fourier transform (FFT) algorithm could be utilized. Before computing the FFT, the time-averaged value of the signal was subtracted from each data point of the oscilloscope trace, and a Hanning window function was applied to the temporal data to reduce leakage effects.[57] Consistent with the use of low-pass filters to minimize aliasing error, the frequency response of the electronic apparatus was tested to be relatively flat up to ~1 MHz. All power spectra shown in this section were corrected for the frequency response of the instruments. The frequency response of the triple probe is expected to be flat up to the ion plasma frequency (~100 MHz) (Ref. 58), which was well beyond the frequencies investigated (<2.5 MHz).

Four general statements can be made about the measurements taken in the plume of the 10-kW thruster. First, turbulent fluctuations were observed only at high values of $J_t^2/\dot{m}$, the minimum value ranged from 40–60 kA^2 s/g. Second, the fluctuating amplitudes of V_{d2} and of the current were often observed to be a significant fraction of the mean values (up to 50%). Third, the power spectra of V_{d2} were essentially identical to that of the current. Finally, the power spectrum measurements obtained in this experiment could be placed into two distinct categories: one consistent with the presence of the GLHDI and the other consistent with the presence of both the GLHDI and the ECDI.

Before showing a sample of the first type of power spectra it is useful to discuss where in frequency space the peaks are expected to occur. To assist in the interpretation of the spectra, the linear characteristics of the microinstabilities are used throughout this section, even though the spectra are turbulent and nonlinear in nature. In actuality, only the peaks in the spectra will be compared with linear theory; no attempt was made to describe their structure. In the ion rest frame, the frequency at which the power spectrum is maximum is expected to be on the same order of frequency corresponding to maximum growth (cf. Table 1). Because the ions are flowing with respect to the triple probe, the peak frequency will be Doppler shifted. The following equation is used to predict the peak frequency in the laboratory frame:

$$f_{lab} = \left| f^* + [\vec{k}^* \cdot \vec{U}_i/2\pi] \right| \tag{1}$$

where $|\ |$ signifies the absolute value, $\vec{U}_i$ is the ion flow vector, and f^* and k^*, respectively, represent the frequency and wavevector corresponding to maximum growth of the instability in the ion rest frame, which are tabulated in Table 1.

For the GLHDI, the maximum temporal growth rate in the ion rest frame, occurs at a frequency near the lower hybrid frequency, but the magnitude and direction of k^* are sensitive to the plasma properties and are not known accurately for the plasma conditions of the 10-kW thruster plume. Of particular interest is an estimate of the largest frequency f_{max} for which the peak in the turbulent spectra is expected to be observed in the laboratory frame. From Eq. (1), it is seen that the largest value of f_{lab} occurs for the largest value of k^*, which corresponds to $k^* r_{Le} \sim 1$ for the GLHDI (cf. Table 1). Substituting into Eq. (1)

$$f_{max} \sim f_{LH} + (U_i/2\pi r_{Le}) \tag{2}$$

where $r_{Le} = V_{te}/\Omega_e$. Equation (1) can be written as

$$\frac{f_{max}}{f_{LH}} \sim 1 + \frac{U_i}{\sqrt{(2\kappa T_e/M_i)}} \tag{3}$$

Note that the ratio $U_i/(2\kappa T_e/M_i)^{1/2}$ is typically 2–4 in the plume of an MPD thruster operating on argon.

The maximum frequency f_{max} can be estimated from experimental measurements using the following method: f_{LH} and r_{Le} are computed from the measured magnetic field and T_e, and the ion flow velocity is estimated from the following relation[1]:

$$U_i = \frac{\mu_0}{4\pi} \ell n \left(\frac{r_a}{r_c}\right) \frac{J_t^2}{\dot{m}} \tag{4}$$

where r_a and r_c are the anode and cathode radius, respectively, and μ_0 is the permeability constant. This expression for the ion flow velocity is consistent with the regime of thruster operation under study (i.e., when the electromagnetic component of thrust is much greater than the electrothermal component), and flow velocity measurements[59] and velocities inferred from

thrust measurements[9] in the 10-kW thruster also agree fairly well with the previous expression (within ~50%).

A sample of the first type of spectra is shown in Fig. 5 for argon. The normalized power spectrum vs frequency is plotted, where the normalized power spectrum is equal to $S_{11}(f)/S_{11}(f_m)$, and f_m is the frequency at which the power spectrum S_{11} is maximum. The scatter in the power spectra, due to the use of discrete Fourier transform techniques, is not physical. The scatter can be reduced by increasing m, which is chosen as a compromise between acceptable statistical scatter and frequency resolution.[49,57] The left-most data point, at ≈5 kHz, represents the average power between ~100 and ≈10 kHz. Each data point thereafter represents the average power between ±5 kHz of the corresponding frequency. In addition, based on the observation of oscillation-free Hall probe measurements, the power spectra is expected to fall off at frequencies less than on the order of 100 Hz. Indicated on the lower frequency scale are the measured natural frequencies of the plasma, and along the top of the plot, f_{max} associated with the GLHDI and $f_{n=1}$ for the ECDI (to be discussed later) are identified. The essential feature of these results is the presence of large-amplitude, naturally occurring turbulent fluctuations near the lower hybrid frequency (which is different from any of the other natural frequencies by at least two orders of magnitude). These spectra are consistent with the presence of the GLHDI in the plume of the 10-kW thruster. Measurements taken in the plume of the 10-kW thruster operating on helium also showed this same phenomenon.[49]

Samples of the second type of power spectra are shown in Figs. 6 and 7. These spectra consist of the same broadband peak near the Doppler-shifted lower hybrid frequency, but with the inclusion of high-power spikes at integral frequencies from each other. These spikes generally occur at much higher frequencies than the Doppler-shifted lower hybrid frequency and are indicative of the ECDI's presence in the plume of the 10-kW thruster. Although difficult to view on a logarithmic scale, this type of spectra is also observed in Fig. 5, with faint peaks at 1 and 2 MHz.

Assuming these spikes are a manifestation of the ECDI, their location in frequency space can be described by the following relation:

$$f_n = \frac{nf_{ce}}{[(U_e/V_{ti}) - 1]} \left| \left(1 - \frac{J}{J}\cdot\frac{U_i}{V_{ti}}\right) \right| \qquad (n = 1, 2, 3, \ldots) \qquad (5)$$

where $V_{ti} = (2\kappa T_i/M_i)^{1/2}$. This expression was obtained by substituting f^* and k^* from Table 1 into Eq. (1), and using the fact that $k \cdot U_e > 0$ is required for the instability to operate. The frequency f_n can be predicted from the measurements of B, J, n_e, and T_e, and by assuming that $T_i = T_e$, estimating the direction of U_i from separate flow angle measurements,[49] and by the use of Eq. (4) to calculate U_i. When $f_{n=1}$ was calculated to be greater than the Nyquist frequency, the high-power spikes were not seen, and when it was predicted that $f_{n=1}$ was less than the Nyquist frequency, the location of the spikes were observed to agree with Eq. (5) within experimental error (which was a factor of 2–3). This evidence suggests that the ECDI is also prominent throughout the near-field plume of the 10-kW thruster ($r \leq 3$ cm, $z < D$).

Finally, it should be stated that no conclusions can be reached about microturbulence occurring near the other natural frequencies, because they were not in the viewing range of the experiment. Furthermore, it is not expected that this turbulence, if it exists, will be consistently Doppler shifted into the viewing range. The Doppler shift of the ion cyclotron harmonics is expected to be too small to be seen in this experiment, because typically k^* is much smaller than the inverse electron gyroradius ($k^* \ll r_{Le}^{-1}$) when the GLHDI is also active.[60] It may also be possible for microturbulence occurring at frequencies near f_{pi} and $(m_e/M_i)^{1/3}f_{pe}$ (in the ion rest frame) to be Doppler shifted into the viewing range of the experiment

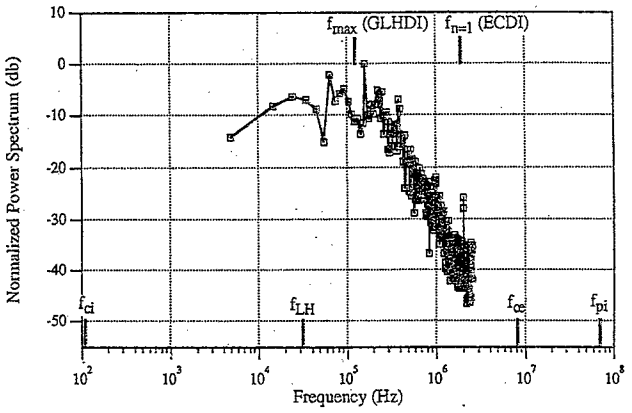

Fig. 5 Comparison of the turbulent power spectrum to measured natural frequencies of the plasma and to the frequencies corresponding to the maximum linear growth rate (argon, J_t = 685 A, $\dot{m}$ = 8 mg/s, r = 1.1 cm, z = 1.6 cm, and m = 4).

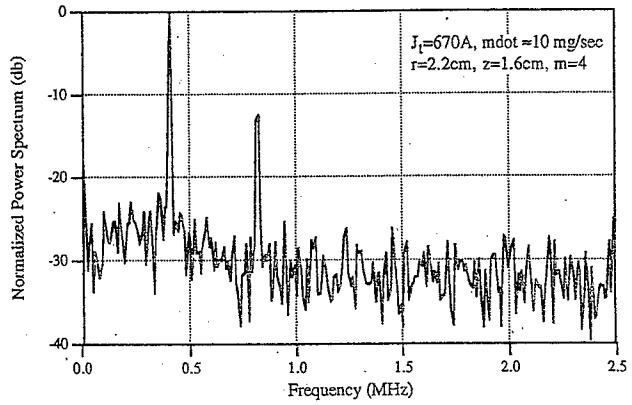

Fig. 6 Sample turbulent power spectrum of the second type obtained in the plume of the 10-kW MPD thruster. This power spectrum indicates the presence of the ECDI (argon, predicted frequencies: f_{max} ~ 190 kHz and $f_{n=1}$ ~ 700 kHz).

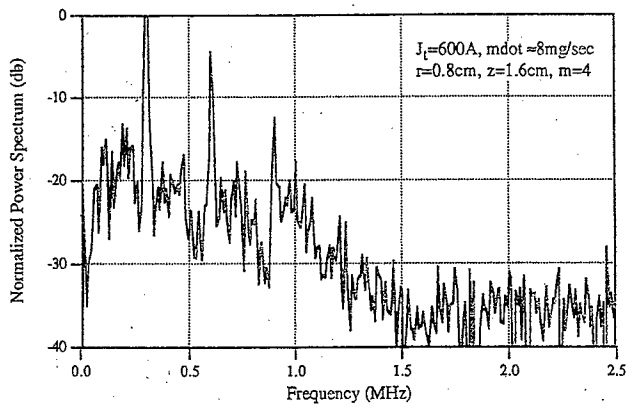

Fig. 7 Sample turbulent power spectrum of the second type obtained in the plume of the 10-kW MPD thruster. This power spectrum indicates the presence of the ECDI (argon, predicted frequencies: f_{max} ~ 70 kHz and $f_{n=1}$ ~ 830 kHz).

if $k^* \cdot U_i < 0$. This is not expected to be observed on a regular basis because for the microinstabilities corresponding to these frequencies: $f_N << f^*$ and $f_N << |k^* \cdot U_i|$.

V. Measurement of the Plasma Dispersion Relation

Large-amplitude, naturally occurring plasma property fluctuations (i.e., plasma turbulence) are the nonlinear, saturated state manifestation of plasma instabilities. For this reason, mi-

croinstabilities in the plume of the 10-kW thruster were identified by comparing only the gross features of the turbulent power spectrum with linear stability theory. A more direct approach in the identification of microinstabilities is to measure the linear dispersion relation, along with the plasma properties required by the linear stability model, and compare the experimental results with theory.

In the plume of the 10-kW thruster, where $\beta_e >> 1$, many practical considerations limit the scope of this type of experiment. Although a linear stability model exists for the MPD thruster plasma for arbitrary β_e (Ref. 29), that theory does not include gradient effects that are expected to be important at high β_e. Furthermore, the accuracy of plasma dispersion relation and plasma property measurements are limited such that a careful comparison of experiment with linear theory would not be fruitful; indeed, the ion temperature and ion flow velocity, required by the model, were not measured at all. Throughout this study, the ion temperature was assumed to be approximately equal to T_e, and U_i has been inferred from Eq. (4). In light of these limitations, it was desired that the results of this experiment would provide an order-of-magnitude type of evidence in support of the presence of the GLHDI and ECDI in the plume of the 10-kW thruster.

The essence of this experiment consists of two Langmuir probes placed a finite distance apart. These probes are biased negative with respect to the plasma potential to measure ion saturation current fluctuations, which are assumed to reflect naturally occurring ion-number density fluctuations only. By measuring the phase difference between the fluctuations at each of the probes, the plasma dispersion relation (i.e., V_ϕ along the line of the probes as a function of frequency) can be derived. Technically, a nonlinear theory is required to describe the phase information obtained from this experiment, but as mentioned earlier, it is commonly observed that saturated-state plasma fluctuations still retain much of their linear characteristics.[56] Along with the plasma dispersion relation measurements, radial profiles of the plasma properties were measured by the thruster-axis-aligned triple probe and the Hall probe.

Two asymmetric double probes, oriented perpendicular to the thruster axis, were used to measure the ion saturation current fluctuations.[49] The two double probes were placed such that the larger electrodes were situated nominally 5 mm apart along the thruster axis, which was the main direction of the electron drift in the 10-kW thruster plume. Across the electrodes of the two probes a fixed bias (nominally ~20 V) ensured that the double probes operated in the ion saturation regime and ac current probes were used to record the ion current fluctuations. Each of these signals was then amplified, filtered (to reduce aliasing error), and recorded on a Nicolet 320 digital oscilloscope sampling at a 2-MHz rate. The data were processed in the same manner as discussed previously.

Measurements were taken at various regions of the plume and at many different thruster operating conditions. It was generally observed that the phase velocity was relatively independent of frequency over the frequency range of 100–500 kHz ($0.7 \leqslant f/f_{LH} \leqslant 10$), which was the region where the measurements were most accurate. Typically, V_ϕ ranged from ≈8 –15 km/s for $50 \leqslant J_t^2/\dot{m}$ (kA^2 s/g) $\leqslant 60$, and from ≈20–30 km/s for $60 \leqslant J_t^2/\dot{m}$ (kA^2 s/g) $\leqslant 90$. The phase velocity was always directed in the $+z$ direction for regions of the plume where $J_z > 0$ and $J_z < 0$.

A typical phase velocity measurement is shown in Fig. 8. The error associated with the phase velocity measurement[61] is due to statistical scatter, aliasing error, and the uncertainty in the phase shift due to the electronics (<5 deg up to 550 kHz). Although the signals of the two probes were very coherent at frequencies less than 500 kHz, the large error at low frequencies was due to the large fractional uncertainty of the frequency and phase shift measurement. At high frequencies (>500 kHz), statistical scatter and aliasing error dominate. The magnitude of V_ϕ and the observation that V_ϕ was relatively constant over the frequency range investigated both compare favorably with the theoretical characteristics of the GLHDI. For the high-β region of the MPD thruster, the phase velocities (in the ion rest frame) are expected to be greater than, but on the order of, the ion thermal velocity ($V_{ti} = 2.2[T_i(eV)]^{1/2}$ km/s for argon) and relatively independent of frequency.[29,43] In the laboratory frame, the phase velocity will be increased by an increment $\boldsymbol{U}_i \cdot \boldsymbol{k}/|\boldsymbol{k}|$, which for the data shown in Fig. 8 is approximately 12 km/s. Assuming $T_i \sim T_e$, the magnitude of the phase velocity is definitely near the theoretically expected values.

Many times the power spectra of the ion current fluctuations, obtained in this experiment, exhibited the same high-power spikes seen in Figs. 6 and 7. In addition, the location of the spikes in the frequency domain were observed to agree with Eq. (5) within experimental error. By investigating the magnitude of V_ϕ associated with these spikes, it was possible to gain further evidence for the existence of the ECDI in the plume of the 10-kW thruster. In theory, the phase velocity (in the ion rest frame) associated with each harmonic of the ECDI is very near the ion thermal velocity. In the laboratory frame, the phase velocity is expressed as

$$V_\phi \cong V_{ti} + U_i \cdot \frac{k}{|k|} \tag{6}$$

This expression, which represents the resonance condition between the energy absorbing ions and the negative-energy Bernstein harmonics,[46] is expected to be very resilient among the different plasma regimes of the MPD thruster. In fact, in its

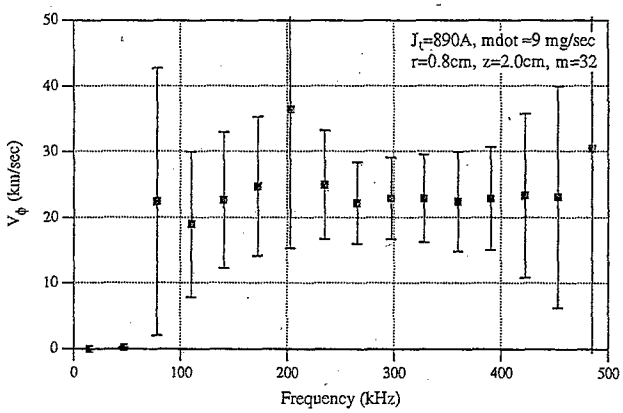

Fig. 8 Typical measurement of the phase velocity in the plume of the 10-kW MPD thruster (argon).

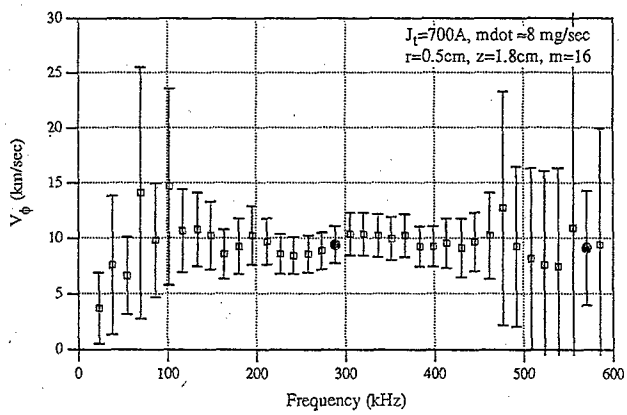

Fig. 9 Typical measurement of the phase velocity in the plume of the 10-kW MPD thruster when the power spectrum exhibited sharp peaks similar to those in Figs. 6 and 7 (argon). The filled circles correspond to the peaks in the power spectrum.

turbulent state, as in this experiment, Eq. (6) is also expected to be valid.[47]

Figure 9 illustrates a typical phase velocity measurement when the high-power spikes were present in the power and cross spectra. The filled circles at the frequencies of 290 and 580 kHz represent the location in frequency space where the spikes were observed. The phase velocity associated with the spikes are ≈9 km/s, which is near theoretical expectations (assuming $T_i \sim T_e$). Phase velocity measurements in agreement with Eq. (6) ($V_\phi \approx 7-12$ km/s) were consistently observed at the frequencies corresponding to the spikes in the power and cross spectra.

In summary, order of magnitude comparisons of linear theory with phase velocity measurements associated with the naturally occurring plasma fluctuations were consistent with the presence of the GLHDI and ECDI in the plume of the 10-kW MPD thruster.

VI. Conclusions

The objective of this research was to provide experimental evidence for the existence of microinstabilities in a 10-kW-class self-field MPD thruster. The lower-bound of the range of thruster operating currents investigated in this study was set by the requirement that the electromagnetic thrust component be much greater than the electrothermal thrust component; the maximum current was limited by the so-called onset current.

Because of the lack of experimental evidence, the theoretical characteristics of many of the microinstabilities that may exist in the self-field MPD thruster were reviewed. It was concluded that two current-driven microinstabilities are suspected to persist throughout the plasma of the self-field MPD thruster: GLHDI and ECDI. From the comparison of the location of peaks in the power spectra (of plasma property oscillations) to the linear theory of the GLHDI and ECDI, experimental evidence for their existence in the plume of the 10-kW-class self-field MPD thruster was obtained. Additional experimental evidence was provided by the measurement of phase velocities associated with these naturally occurring plasma oscillations, which were also observed to be consistent, within experimental error, with the linear theory of the GLHDI and ECDI.

Acknowledgments

This research is supported, in part, by NASA Contract 954997, AFOSR Contract 91-0162, and Grants from Rocket Research, Inc., the U.S. Department of Energy, Plasma Physics Lab, and General Electric Astro, Space Division, Princeton, New Jersey.

References

[1]Jahn, R. G., *The Physics of Electric Propulsion*, McGraw-Hill, New York, 1968.

[2]Sovey, J. S., and Mantenieks, M. A., "Performance and Lifetime Assessment of MPD Arc Thruster Technology," *Journal of Propulsion and Power*, Vol. 7, No. 1, 1991, pp. 71–83.

[3]Choueiri, E. Y., Kelly, A. J., and Jahn, R. G., "Current-Driven Instabilities of an Electromagnetically Accelerated Plasma," 20th International Electric Propulsion Conf., IEPC Paper 88-042, Oct. 1988.

[4]Cap, F., *Handbook on Plasma Instabilities*, Vols. 1 and 2, Academic, New York, 1976, 1978.

[5]Shishkin, G. G., and Gerasimov, V. F., "Plasma Instabilities in Accelerators with Closed Electron Drift," *Soviet Physics—Technical Physics*, Vol. 20, No. 9, 1976, pp. 1171–1174.

[6]Clark, K. E., DiCapua, M. S., Jahn, R. G., and Von Jaskowski, W. F., "Quasi-Steady Magnetoplasmadynamic Arc Characteristics," AIAA Paper 70-1095, Aug. 1970.

[7]Tahara, H., Yasui, H., Kagaya, Y., and Yoshikawa, T., "Experimental and Theoretical Researches on Arc Structure in a Self-Field Thruster," AIAA Paper 87-1093, May 1987.

[8]Turchi, P. J., and Jahn, R. G., "Cathode Region of a Quasi-Steady MPD Arcjet," *AIAA Journal*, Vol. 9, No. 7, 1971, pp. 1372–1379.

[9]Myers, R. M., "Energy Deposition in Low Power Coaxial Plasma Thrusters," Ph.D. Dissertation, Princeton Univ., Princeton, NJ, June 1989; also International Electric Propulsion Conf., IEPC Paper 88-024, Oct. 1988.

[10]Tilley, D. L., Kelly, A. J., and Jahn, R. G., "The Application of the Triple Probe to MPD Thruster Plumes," AIAA Paper 90-2667, July 1990.

[11]Gallimore, A. D., Kelly, A. J., and Jahn, R. G., "Anode Power Deposition in MPD Thrusters," 22nd International Electric Propulsion Conf., IEPC Paper 91-125, Oct. 1991.

[12]Bruckner, A. P., and Jahn, R. G., "Exhaust Plume Structure in a Quasi-Steady MPD Accelerator," *AIAA Journal*, Vol. 12, No. 9, 1974, pp. 1198–1203.

[13]Kilfoyle, D. B., Martinez-Sanchez, M., Heimerdinger, D. J., and Sheppard, E. J., "Spectroscopic Investigation of the Exit Plane of an MPD Thruster," 20th International Electric Propulsion Conf., IEPC Paper 88-027, Oct. 1988.

[14]Shubin, A. P., "Dynamic Nature of Critical Regimes in Steady-State High Current Plasma Accelerators," *Soviet Journal of Plasma Physics*, Vol. 2, No. 1, 1976, pp. 18–21.

[15]Choueiri, E. Y., Kelly, A. J., and Jahn, R. G., "MPD Thruster Plasma Instability Studies," AIAA Paper 87-1067, May 1987.

[16]Murthy, S. N. B., Shoureshi, R., and Pourki, F., "An Approach to MPD Engine Instabilities," AIAA Paper 87-0384, Jan. 1987.

[17]Niewood, E. H., Preble, J., Hastings, D. E., and Martinez-Sanchez, M., "Electrothermal and Modified Two Stream Instability in MPD Thrusters," AIAA Paper 90-2607, July 1990.

[18]Schrade, H. O., Auweter-Kurtz, M., and Kurtz, H. L., "Stability Problems in Magnetoplasmadynamik ARC Thrusters," AIAA Paper 85-1633, July 1985.

[19]Rempfer, D., Auweter-Kurtz, M., Kaeppeler, H. J., and Maurer, M., "Investigation of Instabilities in MPD Thruster Flows Using a Linear Dispersion Relation," 20th International Electric Propulsion Conf., IEPC Paper 88-071, Oct. 1988.

[20]Wagner, H. P., Auweter-Kurtz, M., Roesgen, T., and Kaeppeler, H. J., "Gradient Driven Instabilities in Stationary MPD Thruster Flows," AIAA Paper 90-2603, July 1990.

[21]Wagner, H. P., Auweter-Kurtz, M., Messerschmid, E. W., and Kaeppeler, H. J., "Gradient Influenced Space Charge Instabilities in MPD Thrusters," 22nd International Electric Propulsion Conf., IEPC Paper 91-101, Oct. 1991.

[22]Kuriki, K., and Iida, H., "Spectrum Analysis of Instabilities in MPD Arcjet," 17th International Electric Propulsion Conf., IEPC Paper 84-28, Sept. 1984.

[23]Hassan, H. A., and Thompson, C. C., "Onset of Instabilities in Coaxial Hall Current Accelerators," AIAA Paper 69-230, March 1969.

[24]Smith, J. M., "Electrothermal Instability—An Explanation of the MPD Arc Thruster Rotating Spoke Phenomenon," AIAA Paper 69-231, March 1969.

[25]Abramov, V. A., Vinogradova, A. K., Dontsov, Y. P., Zavenyagin, Y. A., Kovrov, P. E., Kogan, V. I., and Morozov, A. I., "Investigation of Electron Temperature and Plasma Radiation in a Quasi-Stationary High-Current Discharge Between Coaxial Electrodes," *A Survey of Phenomena in Ionized Gases*, International Atomic Energy Agency, Vienna, Austria, 1968, p. 3.1.11.8.

[26]Lovberg, R. H., "Plasma Problems in Electric Propulsion," *Methods of Experimental Physics (Vol. 9): Plasma Physics (Part B)*, edited by Griem and Lovberg, Academic, New York, 1971, pp. 251–289, Chap. 16.

[27]Hastings, D. E., and Niewood, E., "Theory of the Modified Two-Stream Instability in a Magnetoplasmadynamic Thruster," *Journal of Propulsion and Power*, Vol. 7, No. 2, 1991, pp. 258–268.

[28]Choueiri, E. Y., Kelly, A. J., and Jahn, R. G., "Current-Driven Plasma Acceleration Versus Current-Driven Energy Dissipation, Part 1: Wave Stability Theory," AIAA Paper 90-2610, July 1990.

[29]Choueiri, E. Y., "Electron-Ion Streaming Instabilities of an Electromagnetically Accelerated Plasma," Ph.D. Dissertation, Princeton Univ., Princeton, NJ, Oct. 1991.

[30]Choueiri, E. Y., Kelly, A. J., and Jahn, R. G., "Current-Driven Plasma Acceleration Versus Current-Driven Energy Dissipation Part II: Electromagnetic Wave Stability Theory and Experiments," 22nd International Electric Propulsion Conf., IEPC Paper 91-100, Oct. 1991.

[31]Caldo, G., Choueiri, E. Y., Kelly, A. J., and Jahn, R. G., "Numerical Simulation of MPD Thruster Flows with Anomalous Transport," AIAA Paper 92-3738, July 1992.

[32]Choueiri, E. Y., "Current-Driven Plasma Acceleration Versus Current-Driven Energy Dissipation, Part III: Anomalous Transport," AIAA Paper 92-3739, July 1992.

[33]Maurer, M., and Kaeppeler, H. J., "Development of Nonlinear Phenomena Due to Instabilities in MPD-Thruster Flows," AIAA Paper 92-3294, July 1992.

[34]Hsia, J. B., Chu, S. M., Hsia, M. F., Chou, R. L., and Wu, C. S., "Generalized Lower-Hybrid-Drift Instability," *Physics of Fluids*, Vol. 22, No. 9, 1979, pp. 1737–1746.

[35]Lemons, D. S., and Gary, S. P., "Current-Driven Instabilities in a Laminar Perpendicular Shock," *Journal of Geophysical Research*, Vol. 83, No. A4, 1978, pp. 1625–1632.

[36]Wegmann, T., et al., "Experimental Investigation of Steady State High Power MPD Thrusters," AIAA Paper 92-3464, July 1992.

[37]Aref'ev, V. I., "Instability of a Current-Carrying Homogeneous Plasma," *Soviet Physics—Technical Physics*, Vol. 14, No. 11, 1970, pp. 1487–1491.

[38]Buneman, O., "Dissipation of Currents in Ionized Media," *Physical Review*, Vol. 115, No. 3, 1959, pp. 503–517.

[39]Lashmore-Davies, C. N., and Martin, T. J., "Electrostatic Instabilities Driven by an Electric Current Perpendicular to a Magnetic Field," *Nuclear Fusion*, Vol. 13, No. 2, 1973, pp. 193–203.

[40]Priest, E. R., and Sanderson, J. J., "Ion Acoustic Instability in Collisionless Shocks," *Plasma Physics*, Vol. 14, No. 9, 1972, pp. 951–958.

[41]Mikhailovskii, A. B., and Timofeev, A. V., "Theory of Cyclotron Instability in a Non-Uniform Plasma," *Soviet Physics—JETP*, Vol. 17, No. 3, 1963, pp. 626, 627.

[42]Huba, J. D., and Ossakow, S. L., "Destruction of Cyclotron Resonance in Weakly Collisional, Inhomogeneous Plasmas," *Physics of Fluids*, Vol. 22, No. 7, 1979, pp. 1349–1354.

[43]Davidson, R. C., Gladd, N. T., and Wu, C. S., "Effects of Finite Plasma Beta on the Lower-Hybrid-Drift Instability," *Physics of Fluids*, Vol. 20, No. 2, 1977, pp. 301–310.

[44]Wu, C. S., Zhou, Y. M., Tsai, S. T., and Guo, S. C., "A Kinetic Cross-Field Streaming Instability," *Physics of Fluids*, Vol. 26, No. 5, 1983, pp. 1259–1267.

[45]Schmidt, M. J., and Gary, S. P., "Density Gradients and the Farley-Buneman Instability," *Journal of Geophysical Research*, Vol. 78, No. 34, 1973, pp. 8261–8265.

[46]Lashmore-Davies, C. N., "Instability in a Perpendicular Collisionless Shock Wave for Arbitrary Ion Temperatures," *Physics of Fluids*, Vol. 14, No. 7, 1971, pp. 1481–1484.

[47]Galeev, A. A., Lominadze, D. G., Pataraya, A. D., Sagdeev, R. Z., and Stepanov, K. N., "Anomalous Plasma Resistance Due to Instability at Cyclotron Harmonics," *JETP Letters*, Vol. 15, No. 3, 1972, pp. 294–296.

[48]Boyle, M. J., Clark, K. E., and Jahn, R. G., "Flowfield Characteristics and Performance Limitations of Quasi-Steady Magnetoplasmadynamic Accelerators," *AIAA Journal*, Vol. 14, No. 7, 1976, pp. 955–962.

[49]Tilley, D. L., "An Investigation of Microinstabilities in a 10-kW Level Self-Field MPD Thruster," M.S. Thesis, Princeton Univ., Princeton, NJ, Oct. 1991; also International Electric Propulsion Conf., IEPC Paper 91-122, Oct. 1991.

[50]Chamberlain, F. R., "Electropositive Surface Layer MPD Cathodes," M.S. Thesis, Princeton Univ., Princeton, NJ, May 1989; also AIAA Paper 89-2706, July 1989.

[51]Chen, S. L., and Sekiguchi, T., "Instantaneous Direct-Display System of Probe Parameters by Means of Triple Probe," *Journal of Applied Physics*, Vol. 36, No. 8, 1965, pp. 2363–2375.

[52]Lamframboise, J., "Theory of Cylindrical and Spherical Langmuir Probes in a Collisionless Plasma at Rest," Univ. of Toronto, Inst. for Aerospace Studies, VTIAS Rept. 100, June 1966.

[53]Maisenhalder, F., and Mayerhofer, W., "Jet-Diagnostics of a Self-Field Accelerator with Langmuir Probes," *AIAA Journal*, Vol. 12, No. 9, 1974, pp. 1203–1209.

[54]Botticher, W., "Measurement of Magnetic Fields in Plasmas," *Plasma Diagnostics*, edited by W. Lochte-Holtgreven, Wiley, New York, 1968, pp. 617–665.

[55]Zhou, Y. M., Li, Y. Y., and Wu, C. S., "Stabilizing Effects of a Magnetic Field Gradient in a Perpendicular Shock Wave on Electron Cyclotron Drift Instability," *Physics of Fluids*, Vol. 27, No. 8, 1984, pp. 2049–2054.

[56]Ellis, R. F., and Motley, R. W., "Current-Driven Collisional Drift Instability," *Physics of Fluids*, Vol. 17, No. 3, 1974, pp. 582–594.

[57]Smith, D. E., Powers, E. J., and Caldwell, G. S., "Fast-Fourier-Transform Spectral Analysis Techniques as a Plasma Fluctuation Diagnostic Tool," *IEEE Transactions on Plasma Science*, Vol. PS-2, No. 2, 1974, pp. 261–272.

[58]Chen, F. F., "Electric Probes," *Plasma Diagnostic Techniques*, edited by R. H. Huddlestone and S. L. Leonard, Academic, New York, 1965, pp. 113–200.

[59]Diamant, K. D., Tilley, D. L., Choueiri, E. Y., Kelly, A. J., and Jahn, R. G., "MPD Thruster Exhaust Velocity Measurement Using Injected Plasma Waves," 22nd International Electric Propulsion Conf., IEPC Paper 91-049, Oct. 1991.

[60]Diamond, P. H., Myra, J. R., and Aamodt, R. E., "Suppression of the Drift-Cyclotron Instability by Lower-Hybrid-Drift Turbulence," *Physics of Fluids*, Vol. 25, No. 11, 1982, pp. 2005–2011.

[61]Tilley, D. L., Princeton Univ., Mechanical and Aerospace Engineering Rept. 1776.27, Princeton, NJ, 1990.